Stimulation Artifact Source Separation (SASS) for assessing electric brain oscillations during transcranial alternating current stimulation (tACS)

David Haslacher[1], Khaled Nasr[1], Stephen E. Robinson[2], Christoph Braun[3,4], and Surjo R. Soekadar[1,5]*

[1] Clinical Neurotechnology Lab, Neuroscience Research Center (NWFZ), Department of Psychiatry and Psychotherapy, Charité – University Medicine Berlin, Berlin, Germany

[2]National Institute of Mental Health (NIMH), MEG Core Facility, Bethesda, USA

[3]MEG Center, University of Tübingen, Germany

[4]CIMeC, Center of Mind/Brain Sciences, University of Trento, Italy

[5]Applied Neurotechnology Lab, Department of Psychiatry and Psychotherapy, University Hospital of Tübingen, Germany

* Correspondence to: Surjo R. Soekadar, MD, Clinical Neurotechnology Lab, Neuroscience Research Center (NWFZ), Department of Psychiatry and Psychotherapy, Charité – University Medicine Berlin, Charitéplatz 1, 10117 Berlin, Germany. Email: surjo.soekadar@charite.de

Keywords: brain oscillations, single-trial, transcranial alternating current stimulation (tACS), stimulation artifact, electroencephalography (EEG)

Highlights:

- Stimulation Artifact Source Separation (SASS), a real-time-compatible signal decomposition algorithm for separating electric brain activity and stimulation signal artifacts related to amplitude-modulated transcranial alternating current stimulation (AM-tACS), is introduced.

- Employing SASS, phase and amplitude of steady state visually evoked potentials (SSVEPs) were reliably recovered from electroencephalography (EEG) recordings
- SASS paves the way for online adaptation of stimulation parameters to ongoing brain oscillatory activity

Abstract

Brain oscillations, e.g. measured by electro- or magnetoencephalography (EEG/MEG), are causally linked to brain functions that are fundamental for perception, cognition and learning. Recent advances in neurotechnology provide means to non-invasively target these oscillations using amplitude-modulated transcranial alternating current stimulation (AM-tACS). However, online adaptation of stimulation parameters to ongoing brain oscillations remains an unsolved problem due to stimulation artifacts that impede such adaptation, particularly at target frequencies. Here, we introduce a real-time compatible artifact rejection algorithm (Stimulation Artifact Source Separation, SASS) that overcomes this limitation. SASS is a spatial filter (linear projection) removing EEG signal components that are maximally different in the presence versus absence of stimulation. This enables the reliable removal of stimulation-specific signal components, while leaving physiological signal components unaffected. For validation of SASS, we evoked brain activity with known phase and amplitude using 10 Hz visual flickers. 64-channel EEG was recorded during and in absence of 10 Hz AM-tACS targeting the visual cortex. Phase differences between AM-tACS and the visual stimuli were randomized, so that steady-state visually evoked potentials (SSVEPs) were phase-locked to the visual stimuli but not to the AM-tACS signal. For validation, inter-trial phase-locking value (PLV) and mean amplitude of single-trial EEG signals recorded during and in absence of AM-tACS were compared. When no artifact rejection method was applied, AM-tACS stimulation artifacts impeded reconstruction of SSVEP amplitude and phase. Using SASS, PLV and mean amplitudes of single-trial EEG signals recorded during and in absence of

AM-tACS were comparable. These results indicate that SASS can be used to establish adaptive (closed-loop) AM-tACS, a potentially powerful tool to target various brain functions and to investigate how AM-tACS interacts with electric brain oscillations.

1. Introduction

Brain oscillations reflect neuronal cell-assembly formation causally linked to various brain functions, such as perception (Fries, Schroder, Roelfsema, Singer, & Engel, 2002; Hipp, Engel, & Siegel, 2011; Rodriguez et al., 1999), cognition (Kahana, Sekuler, Caplan, Kirschen, & Madsen, 1999), memory (Fell et al., 2001) and learning (Miltner, Braun, Arnold, Witte, & Taub, 1999; Seager, Johnson, Chabot, Asaka, & Berry, 2002). While building on fine-tuned neurochemical processes at the cellular level, brain oscillations were found to be closely related to cortico-cortical communication at the neural circuit and system level (Kopell, Ermentrout, Whittington, & Traub, 2000; Roelfsema, Engel, Konig, & Singer, 1997). As such, brain oscillations assessed by electro- or magnetoencephalography (EEG/MEG) may represent a valuable target to treat neurological and psychiatric disorders in which phase synchronization and large-scale integration is disturbed, e.g. Parkinson's disease, depression or schizophrenia.

A well-established tool to non-invasively target oscillatory brain activity uses transcranial alternating currents specifically tuned to physiological frequencies, e.g. in the alpha (8-15 Hz) or beta band (15-30 Hz). When targeting such frequencies, distinct effects on perception (Helfrich et al., 2014; Thut et al., 2017), movement (Wach et al., 2013), memory (Reinhart & Nguyen, 2019) or emotion regulation (Clancy et al., 2018) were demonstrated. While very promising in its application (Helfrich et al., 2014; Thut, Schyns, & Gross, 2011), tuning of stimulation parameters other than frequency (e.g. phase, intensity, and spatial distribution of the electric fields using multi-electrode montages) was unfeasible up to now because large non-linear stimulation artifacts impede reliable reconstruction of physiological brain activity. This not only limits effective targeting of ongoing brain oscillations, but also the possibility

to systematically investigate how tACS interacts with endogenous rhythmic brain activity, a critical prerequisite to develop new and effective adaptive closed-loop brain stimulation protocols.

Recently, we have introduced a novel tACS approach that uses amplitude modulation of a high frequency carrier signal (e.g. 220 Hz) to reduce stimulation-related artifacts at the lower physiological frequency bands (Witkowski et al., 2016). By modulating the carrier signal's amplitude at a physiological frequency (target frequency), specific brain functions could be influenced, e.g. working memory performance when targeting frontal midline theta (FMT) oscillations (Chander et al., 2016). This finding was corroborated by computational simulations showing that AM-tACS leads to phase-locking of cortical oscillations with the stimulation signal and suggests that AM-tACS exhibits the same target engagement mechanism as conventional (unmodulated) low frequency tACS (Negahbani, Kasten, Herrmann, & Fröhlich, 2018).
Although AM-tACS can substantially reduce stimulation artifact contamination of the physiological frequency bands, intermodulation distortions (IMD) and non-linear interactions related to heartbeat and breathing can introduce stimulation artifacts (Kasten, Negahbani, Fröhlich, & Herrmann, 2018) that could be mistaken as neural entrainment.
Although tACS-artifact suppression strategies have been proposed (Helfrich et al., 2014), there is currently no real-time compatible approach available that allows for adaptive tACS. For this, reliable trial-by-trial reconstruction of relevant physiological signal features, such as amplitude and phase, particularly at the target frequency, is critical.

Here, we introduce Stimulation Artifact Source Separation (SASS), a real-time-compatible signal decomposition algorithm, that allows for separating electric brain activity and AM-tACS-related stimulation artifacts. To test validity and reliability of SASS, brain oscillations with known amplitude and frequency were evoked using a 10 Hz steady-state visual evoked potential (SSVEP) paradigm. Brain

oscillations were recorded by 64-channel EEG while 10-Hz AM-tACS was applied over the visual cortex. While the AM-tACS signal's phase was known, phase of the SSVEPs was randomly distributed and independent of the AM-tACS signal. Assuming that SASS effectively suppresses AM-tACS-related stimulation artifacts at the target frequency, we expected that inter-trial phase-locking values (PLVs) and mean amplitude of single-trial EEG signals would be comparable in the absence of and during AM-tACS.

2. Material and Methods

2.1 Electroencephalography (EEG)

A 64-channel EEG system (Bittium Corp., Oulu, Finland) with passive Ag/AgCl electrodes (Brain Products GmbH, Gilching, Germany) was used to record electrical activity on the scalp. The amplifier was set to DC-mode with a dynamic range of +/-430 V. Electrode impedances were kept below 10 kOhm. Signals were sampled at 2000 Hz with an anti-aliasing filter applied at 500 Hz. Saturated electrodes were excluded from the analysis. Electrodes exhibiting broadband power more than an order of magnitude higher than the median were excluded from the analysis.

2.2 Transcranial alternating current stimulation (tACS)

tACS was applied to the scalp using a commercial stimulator (NeuroConn GmbH, Ilmenau, Germany). Rubber electrodes with a 4 x 5 cm size were placed over position CPz and below Oz according to the 10-20 system. This corresponds to the standard montage used for targeting the visual system during tACS experiments (e.g., Helfrich et al., 2014). The stimulator delivered AM-tACS with a 500 Hz carrier and 10 Hz envelope signal. Stimulation intensity was set to a peak amplitude of 2 mA.

2.3 Presentation of visual flickers

During ongoing AM-tACS, a sinusoidal grating that flickered at 10 Hz was presented for 2 seconds across trials. A random inter-trial interval between 0.5 to 1 second ensured that the onset time of the visual flicker was randomly distributed over the phase of the AM-tACS signal. Visual stimuli were presented via a head-mounted display (Oculus VR Inc., California, USA). Its analog audio output was fed into a bipolar channel of the EEG amplifier and stored to obtain a trigger marker of the stimulus onset time. Jitter between the audio output signal and visual stimulus presentation was under 5 ms. Before the experiment, signal artifacts related to the use of the head-mounted display were ruled out.

2.4 Participants and sessions

Seven healthy participants (4 male, 3 female, 22 - 28 years old) were invited to participate in the study and provided written informed consent. The study was approved by the ethics committee of the Charité – University Medicine Berlin (EA1/077/18). Initially, a calibration session consisting of 100 trials of visual flicker was recorded in absence of AM-tACS. The experimental session consisted of two runs. During the first run, 100 trials of visual flickers were recorded while AM-tACS was applied. During the second run, the same number of trials were performed, during which participants viewed a stationary (non-flickering) grating. Therefore (as per parameters listed in section 2.3), recording time for each condition amounted to approximately 4,5 minutes (275 seconds).

2.5 EEG data preprocessing

MNE-Python (Gramfort et al., 2013) was used for the entire analysis. Oversampled temporal projection (OTP) (Larson & Taulu, 2018) was applied to all raw EEG data to remove uncorrelated sensor noise before any further signal processing. OTP projects sensor data on the (temporal) subspace spanned by its

neighbors in a windowed manner. EEG data were then bandpass filtered at 1 – 15 Hz using FIR filters designed via the Hamming window method (Saramaeki, Mitra, & Kaiser, 1993). Data underlying the EEG signal covariance matrix was bandpass filtered at 9 – 11 Hz.

2.6 Stimulation Artifact Source Separation (SASS)

SASS identifies hidden and linearly separable data components that are maximally attributable to stimulation and least attributable to brain activity. These components are then rejected to achieve artifact suppression. SASS is based on an eigenvalue decomposition of the respective covariance matrices. When performing an eigenvalue decomposition based on a single covariance matrix only, the resulting components are ordered by the amount of variance they explain (principal component analysis). While using only one covariance matrix could be useful for artifact suppression, because most of the variance in the data relates to stimulation artifacts, such an approach does not account for the topography of brain activity and is additionally constrained by the assumption that artifact and brain signal subspaces are orthogonal (limiting the possible subspaces and components to be rejected). SASS is therefore designed to identify components that jointly maximize the variance attributable to stimulation artifacts and minimize the variance attributable to brain activity. This is achieved by calculating the generalized eigenvalues of two covariance matrices. A source separation matrix is computed from the joint diagonalization (generalized eigenvalue problem) of EEG sensor covariance matrices (A) during and (B) in absence of AM-tACS, respectively:

$$W = \begin{pmatrix} w_1{}^T \\ \vdots \\ w_n{}^T \end{pmatrix} \quad \text{where} \quad Aw_i = \lambda_i B w_i \quad \text{and} \quad \lambda_i = \frac{w_i^T A w_i}{w_i^T B w_i}$$

The ratio λ_i represents the degree to which signal variance in component i is attributable to stimulation artifacts rather than brain activity. The source separation matrix W was used to linearly separate the sensor data into components ordered by this ratio. For each participant, components with a robust z-statistics (computed from the distribution of all eigenvalues) exceeding a one-tailed 1% alpha level were rejected. As a last step, the resulting data was projected back into EEG sensor space. The entire procedure can be summarized in a single linear projection:

$$P = W^{+}SW \quad \text{where} \quad S = \begin{pmatrix} 0 & & \\ & \ddots & \\ & & 1 \end{pmatrix} \quad \text{and} \quad W^{+} \text{ denotes the pseudoinverse of } W$$

This projection was applied to the 1 – 15 Hz data that was then epoched into individual trials from which all outcome measures were computed. To minimize the mean squared error in the EEG power spectrum due to slow changes in stimulation artifact topography, the covariance matrix A and subsequent SASS were updated every 60 sec. of EEG data recorded with AM-tACS, while covariance matrix B was kept constant.

2.6 Amplitude and phase of brain oscillations

EEG data of occipital electrodes at positions O1, O2, PO7, PO3, POZ, PO4, and PO8 (according to the international 10/20 system) were evaluated for each electrode separately and as an average across all channels. A 10-Hz sine wave was fit to each epoch. Mean single-trial amplitude and inter-trial phase locking value (PLV) (Lachaux, Rodriguez, Martinerie, & Varela, 1999) were computed for each participant.

2.7 Mean squared error of power spectra

To calculate power spectra, the Welch method was applied using 8192 fast Fourier transform (FFT) points. Power spectra were computed in absence of AM-tACS, during AM-tACS without SASS, and during AM-tACS with SASS. Additionally, the mean squared error of the power spectrum (relative to power recorded in absence of AM-tACS) was calculated before and after SASS.

2.8 Statistical procedures

To test for differences in PLV, amplitude, and mean-squared error of power spectra, one-sided two-sample t-tests were performed. All values were log-transformed to handle outliers. To test for equivalence of PLV and amplitude across conditions (i.e., in absence and during AM-tACS), one-sided one-sample (non-inferiority) t-tests with an accepted mean deviation of 25% in PLV and amplitude were performed.

3. Results

3.1 Visual flicker-entrained occipital brain oscillations

Figure 1 shows SSVEPs in occipital EEG while visual flickers were presented. The amplitude of single-trial 10 Hz activity in occipital channels ($M = 3.63e\text{-}6$, $SD = 1.51e\text{-}6$) was significantly higher, $t(6) = -2.77$, $p < 0.05$, than in absence ($M = 2.17e\text{-}6$, $SD = 6.92e\text{-}7$) of visual flickers.

3.2 SASS recovered the power spectrum and topography of electric brain oscillations

Figure 2A,B shows that sufficient AM-tACS artifact suppression was achieved so that the power spectrum and topography of endogenous brain oscillations were recovered. Without applying SASS, AM-tACS-related artifacts exceed the physiological brain activity by several orders of magnitude. During AM-tACS in absence of visual flickers (Fig. 2A), the mean squared error in the EEG power

spectrum (M = 3.54e-23, SD = 6.98e-23) is notably reduced when SASS is applied compared to when it's not (M = 2.05e-10, SD = 4.76e-10), t(6) = 5.77, p < 0.001). Likewise, during AM-tACS in the presence of visual flickers (Fig. 2B), the mean squared error in the EEG power spectrum was notably reduced (M = 3.00e-23, SD = 3.62e-23) when SASS was applied compared to when it was not (M = 2.17e-10, SD = 5.21e-10), t(6) = 6.55, p < 0.001.

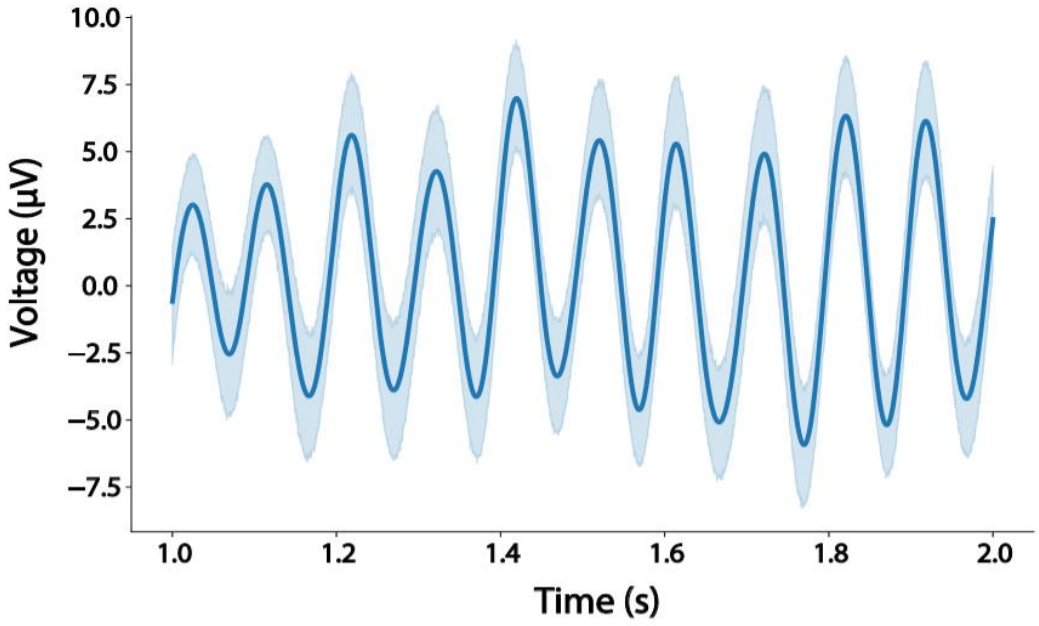

Figure 1: Steady-state visual evoked potentials (SSVEPs). Occipital electroencephalography (EEG) sensors in a representative participant showed characteristic visual evoked potentials at 10 Hz that are locked to the onset of the visual stimuli.

Of note, a clear peak in the power spectrum at 10 Hz remained due to visual stimuli presented at 10 Hz. Moreover, during AM-tACS in presence of 10 Hz visual flickers, the topography of SSVEP amplitudes was completely masked by stimulation artifacts, but recovered by applying SASS. Using SASS, the SSVEP topography during AM-tACS (as quantified as mean squared error, M = 1.88e-13, SD = 1.78e-13) was equivalent to the topography of SSVEPs in the absence of stimulation (M = 4.45e-9, SD = 7.66e-9), t(6) = 6.72, p < 0.001.

A

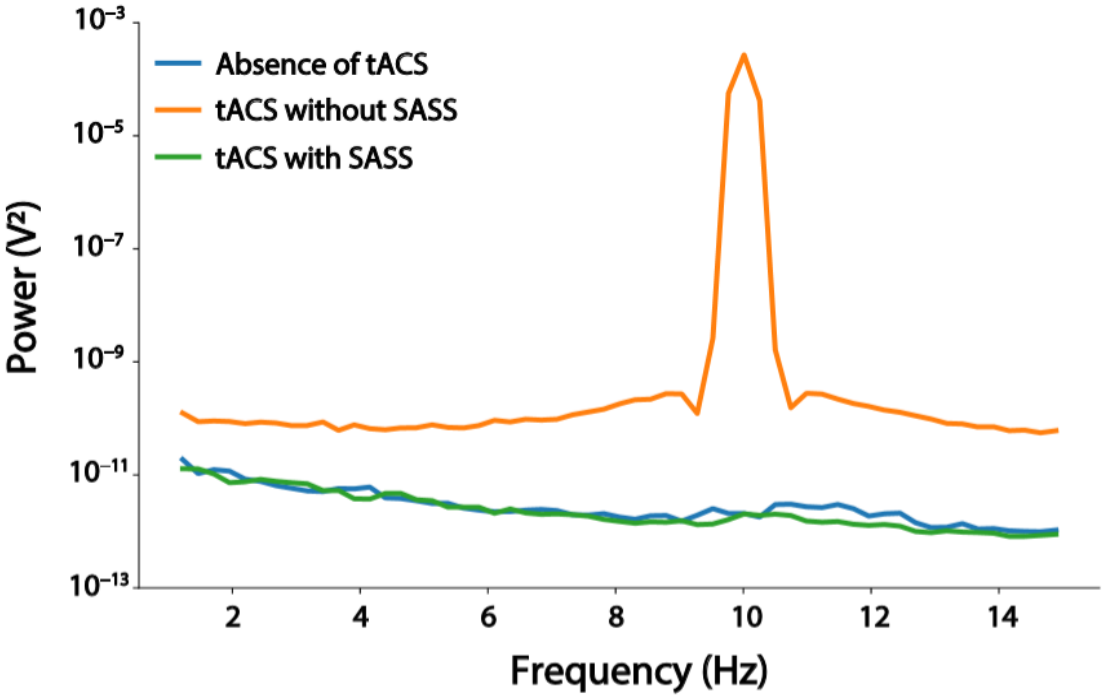

B

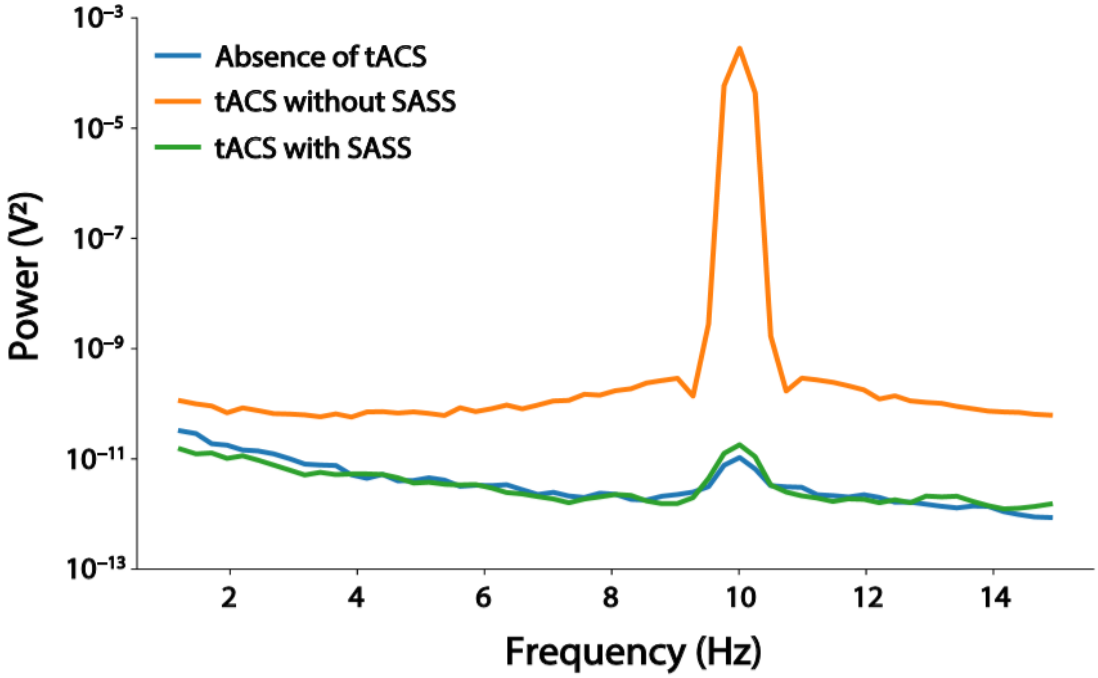

C

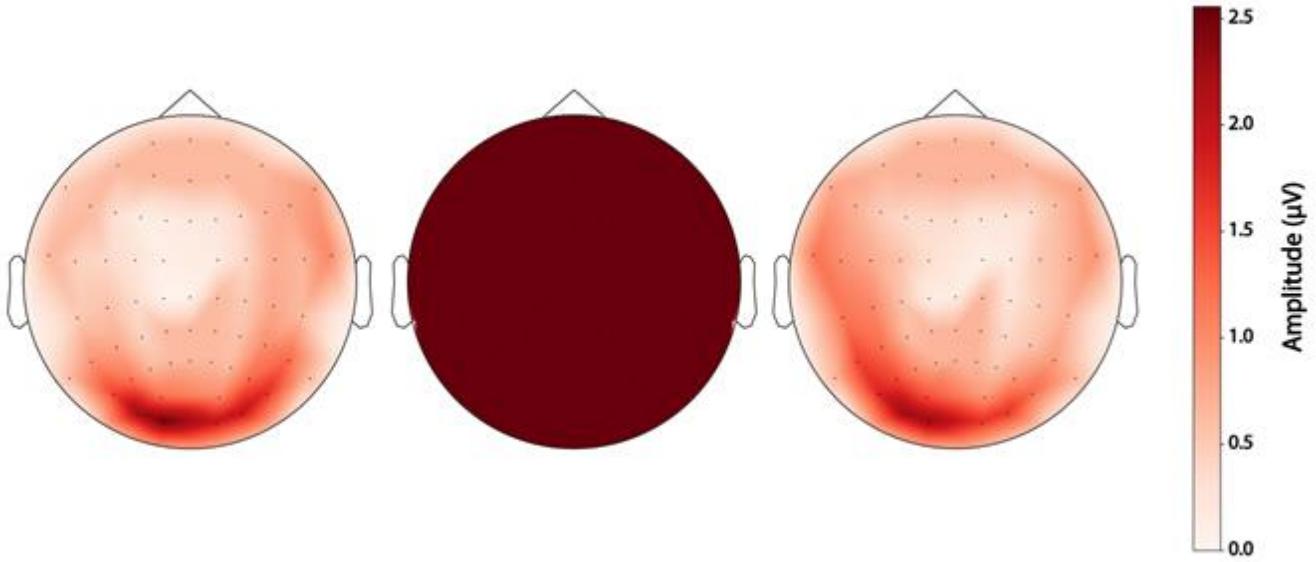

Figure 2: Occipital brain activity is recovered by artifact suppression. A: In absence of visual stimulation, AM-tACS artifacts obscure electric brain activity. Using SASS, the EEG power spectrum during AM-tACS was comparable to the EEG power spectrum in absence of AM-tACS. B: During presentation of visual flickers, AM-tACS artifacts masked occipital brain activity, including SSVEPs. Using SASS, SSVEPs were recovered. C: Left panel: Topography of SSVEP amplitude with a maximum at the occipital pole; Middle panel: Physiological activity is masked by AM-tACS artifacts; Right panel: Using SASS results in recovery of the SSVEP topography.

3.3 SASS recovered amplitude and phase of electric brain oscillations

Figure 3 depicts recovery of SSVEP-related amplitude and phase information of single-trial electric brain oscillations across occipital EEG channels when using SASS during AM-tACS. In absence of AM-tACS, occipital EEG signals showed SSVEPs with a mean PLV of 0.529 (SD = 0.140), and a mean single-trial amplitude of 3.63e-6 V (SD = 1.51e-6). During AM-tACS, PLV decreased, $t(6) = 8.33$, $p < 0.001$, to a mean of 0.110 (SD = 0.147), with the amplitude increasing, $t(6) = -4.45$, $p < 0.01$, to a mean of 1.59e-3 V (SD = 2.63e-3), indicating that electric brain oscillations were obscured by AM-tACS artifacts. When applying SASS, PLV (M = 0.481, SD = 0.147) was not different from PLV recorded in absence of AM-tACS, $t(6) = 0.837$, $p = 0.217$. Testing for equivalence confirmed that there was no difference in PLV across conditions (AM-tACS with SASS and absence of SASS), $t(6) = -2.23$ $p < 0.05$. Similarly, when

applying SASS, SSVEP amplitudes recorded during AM-tACS (M = 3.87e-6, SD = 1.56e-6) were not different from SSVEP amplitudes recorded in absence of AM-tACS, $t(6) = -0.859$, $p = 0.212$. Testing for equivalence confirmed that there was no difference in amplitude across conditions (AM-tACS with SASS and absence of SASS), $t(6) = 2.42$, $p < 0.05$.

A

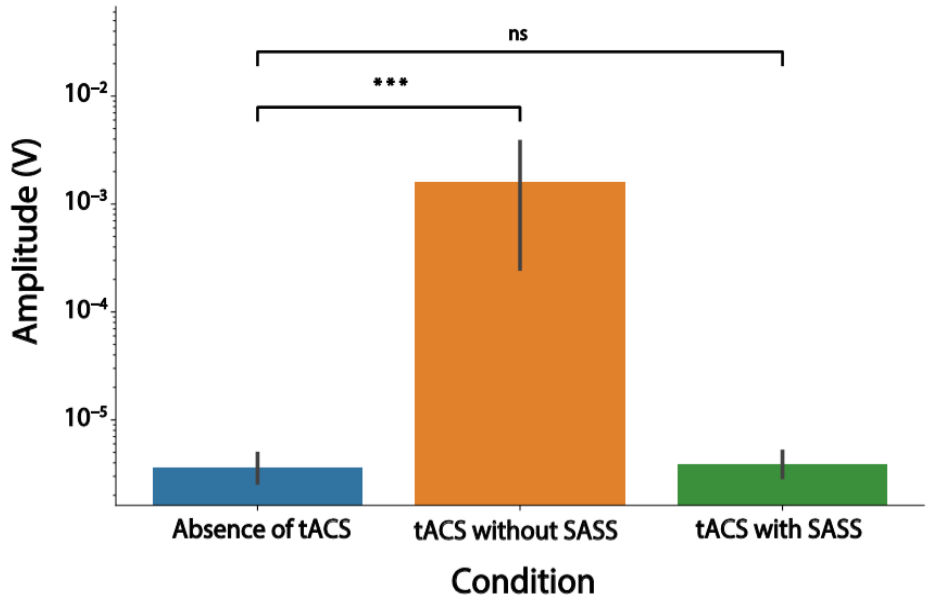

B

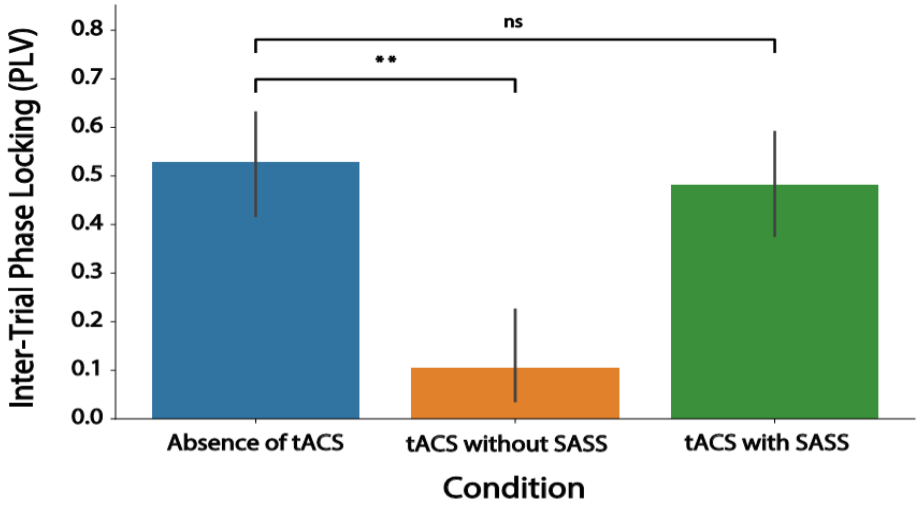

Figure 3: Phase and amplitude of single-trial steady-state visual evoked potentials (SSVEPs) in absence and during AM-tACS. A: Amplitude of SSVEPs is masked by AM-tACS artifacts exceeding electric brain oscillations by several orders of magnitude (orange bar). Using SASS (green bar), SSVEP amplitudes recorded during AM-tACS were comparable to SSVEP amplitudes recorded in absence of AM-tACS. B: Phase information of brain oscillations as measured by inter-trial phase locking value (PLV) is masked by AM-tACS (orange bar). Using SASS (green bar), PLV of evoked brain responses recorded during AM-tACS were comparable to PLV of evoked brain responses recorded in absence of AM-tACS.

4. Discussion

Up to now, there was no real-time compatible signal processing tool available to suppress AM-tACS stimulation artifacts to a degree that allows for recovering phase and amplitude of evoked brain responses at a single-trial level. Here, we introduced SASS, a spatial filter based on a source separation matrix computed from joint diagonalization of EEG sensor covariance matrixes recorded in absence and during AM-tACS. To evaluate the effectiveness of SASS, we used an SSVEP paradigm resulting in evoked brain oscillatory responses with known frequency, amplitude and phase. Electric brain activity was assessed using EEG across seven healthy volunteers in absence and during 10 Hz AM-tACS delivery. Using SASS, SSVEP amplitude and phase information (as measured by inter-trial PLV) was equivalent during AM-tACS and in absence of stimulation (Fig. 3). Moreover, SSVEP topography during AM-tACS resembled SSVEP topography recorded in absence of AM-tACS. Besides showing that SASS is an effective tool for separating electric brain activity and stimulation artifacts, our results pave the way towards implementation of adaptive stimulation paradigms in which the phase, amplitude and the spatial distribution of the stimulation's electric fields become adapted to ongoing brain oscillations. This may contribute to the development of more effective stimulation approaches to target various brain functions and further elucidate the underlying mechanisms of AM-tACS effects.

Due to the design of SASS, it cannot be ruled out that also non-artifact-related signal components, e.g. physiological components modulated by AM-tACS, are attenuated. This is rather unlikely, however,

because signal components are suppressed only if they exceed normal variability of brain oscillations with 99% confidence (section 2.6). While using this alpha level for identifying and attenuating signal components affected by stimulation artifacts was sufficient to recover SSVEP amplitude and phase during stimulation, choosing a less conservative approach may prove advantageous when investigating a particular *a priori* hypothesis related to the underlying mechanisms of AM-tACS effects. Given that SSVEP amplitude and phase was successfully recovered during stimulation, SASS now allows for further investigating AM-tACS-related network effects (Alekseichuk et al., 2019; Reinhart & Nguyen, 2019). SASS could also be used to purposefully modulate large-scale synchronization (Reinhart & Nguyen, 2019) by targeting one cortical region as a function of another. Moreover, SASS may also contribute to further elucidating the underlying mechanisms of tACS effects. Recent studies suggest that tACS effects are not only mediated by electric field-dependent modulations of membrane potentials in superficial cortical layers, but may also involve transcutaneous stimulation of skin nerves (Asamoah, Khatoun, & Mc Laughlin, 2019). Here, SASS may help to identify the primary mechanism of action based on precise characterization of phase locking and phase lags in combination with other neurophysiological measures such as neural conduction times.

Real-time phase estimation of ongoing brain oscillations is challenging and critically depends on the signal-to-noise ratio and instantaneous amplitude of the signal (Zrenner et al., 2020). It is thus important to note that successful implementation of adaptive AM-tACS not only requires real-time suppression of stimulation artifacts, but also stable phase estimation accuracy. This could be achieved by purposefully amplifying the target oscillation's amplitude using a cognitive task (e.g. motor imagery to increase μ-rhythm amplitude) (Soekadar, Witkowski, Birbaumer, & Cohen, 2015; Soekadar, Witkowski, Cossio, Birbaumer, & Cohen, 2014), sensory stimuli (e.g. visual flickers or vibrotactile stimulation), or operant conditioning (e.g. neurofeedback) (Ruddy et al., 2018).

Data availability

The data is publicly available on Mendeley Data: https://data.mendeley.com/datasets/39n9zttp4t.

The implementation of the novel algorithm (termed Stimulation Artifact Source Separation, SASS) is publicly available on GitHub: https://github.com/davidhaslacher/sass.

Disclosures

None.

Credit authorship contribution statement

D.H., K.N., S.R.S., C.B. and S.E.R. were involved in the design of study, analysis and/or interpretation of data, drafting the manuscript, and revising the manuscript critically for important intellectual content. D.H. and K.N. acquired the data.

Acknowledgements

This work was supported in part by the European Research Council (ERC) under the project NGBMI (759370), the Baden-Württemberg Stiftung (NEU007/1) and Einstein Stiftung Berlin. SRS received special support by the Brain & Behavior Research Foundation as 2017 NARSAD Young Investigator Grant recipient and P&S Fund Investigator. We'd like to thank Joel Aftreth for his valuable feedback on this work.

5. References

Alekseichuk, I., Falchier, A. Y., Linn, G., Xu, T., Milham, M. P., Schroeder, C. E., & Opitz, A. (2019). Electric field dynamics in the brain during multi-electrode transcranial electric stimulation. *Nat Commun, 10*(1), 2573. doi:10.1038/s41467-019-10581-7

Asamoah, B., Khatoun, A., & Mc Laughlin, M. (2019). tACS motor system effects can be caused by transcutaneous stimulation of peripheral nerves. *Nat Commun, 10*(1), 266. doi:10.1038/s41467-018-08183-w

Chander, B. S., Witkowski, M., Braun, C., Robinson, S. E., Born, J., Cohen, L. G., . . . Soekadar, S. R. (2016). tACS Phase Locking of Frontal Midline Theta Oscillations Disrupts Working Memory Performance. *Front Cell Neurosci, 10*, 120. doi:10.3389/fncel.2016.00120

Clancy, K. J., Baisley, S. K., Albizu, A., Kartvelishvili, N., Ding, M., & Li, W. (2018). Lasting connectivity increase and anxiety reduction via transcranial alternating current stimulation. *Soc Cogn Affect Neurosci, 13*(12), 1305-1316. doi:10.1093/scan/nsy096

Fell, J., Klaver, P., Lehnertz, K., Grunwald, T., Schaller, C., Elger, C. E., & Fernandez, G. (2001). Human memory formation is accompanied by rhinal-hippocampal coupling and decoupling. *Nat Neurosci, 4*(12), 1259-1264. doi:10.1038/nn759

Fries, P., Schroder, J. H., Roelfsema, P. R., Singer, W., & Engel, A. K. (2002). Oscillatory neuronal synchronization in primary visual cortex as a correlate of stimulus selection. *J Neurosci, 22*(9), 3739-3754. doi:20026318

Gramfort, A., Luessi, M., Larson, E., Engemann, D. A., Strohmeier, D., Brodbeck, C., . . . Hämäläinen, M. (2013). MEG and EEG data analysis with MNE-Python. *Front Neurosci, 7*, 267. doi:10.3389/fnins.2013.00267

Helfrich, R. F., Schneider, T. R., Rach, S., Trautmann-Lengsfeld, S. A., Engel, A. K., & Herrmann, C. S. (2014). Entrainment of brain oscillations by transcranial alternating current stimulation. *Curr Biol, 24*(3), 333-339. doi:10.1016/j.cub.2013.12.041

Hipp, J. F., Engel, A. K., & Siegel, M. (2011). Oscillatory synchronization in large-scale cortical networks predicts perception. *Neuron, 69*(2), 387-396. doi:10.1016/j.neuron.2010.12.027

Kahana, M. J., Sekuler, R., Caplan, J. B., Kirschen, M., & Madsen, J. R. (1999). Human theta oscillations exhibit task dependence during virtual maze navigation. *Nature, 399*(6738), 781-784. doi:10.1038/21645

Kasten, F. H., Negahbani, E., Fröhlich, F., & Herrmann, C. S. (2018). Non-linear transfer characteristics of stimulation and recording hardware account for spurious low-frequency artifacts during amplitude modulated transcranial alternating current stimulation (AM-tACS). *Neuroimage, 179*, 134-143. doi:10.1016/j.neuroimage.2018.05.068

Kopell, N., Ermentrout, G. B., Whittington, M. A., & Traub, R. D. (2000). Gamma rhythms and beta rhythms have different synchronization properties. *Proc Natl Acad Sci U S A, 97*(4), 1867-1872. doi:10.1073/pnas.97.4.1867

Lachaux, J. P., Rodriguez, E., Martinerie, J., & Varela, F. J. (1999). Measuring phase synchrony in brain signals. *Hum Brain Mapp, 8*(4), 194-208. doi:10.1002/(sici)1097-0193(1999)8:4<194::aid-hbm4>3.0.co;2-c

Larson, E., & Taulu, S. (2018). Reducing Sensor Noise in MEG and EEG Recordings Using Oversampled Temporal Projection. *IEEE Trans Biomed Eng, 65*(5), 1002-1013. doi:10.1109/TBME.2017.2734641

Miltner, W. H., Braun, C., Arnold, M., Witte, H., & Taub, E. (1999). Coherence of gamma-band EEG activity as a basis for associative learning. *Nature, 397*(6718), 434-436. doi:10.1038/17126

Negahbani, E., Kasten, F. H., Herrmann, C. S., & Fröhlich, F. (2018). Targeting alpha-band oscillations in a cortical model with amplitude-modulated high-frequency transcranial electric stimulation. *Neuroimage, 173*, 3-12. doi:10.1016/j.neuroimage.2018.02.005

Reinhart, R. M. G., & Nguyen, J. A. (2019). Working memory revived in older adults by synchronizing rhythmic brain circuits. *Nat Neurosci, 22*(5), 820-827. doi:10.1038/s41593-019-0371-x

Rodriguez, E., George, N., Lachaux, J. P., Martinerie, J., Renault, B., & Varela, F. J. (1999). Perception's shadow: long-distance synchronization of human brain activity. *Nature, 397*(6718), 430-433. doi:10.1038/17120

Roelfsema, P. R., Engel, A. K., Konig, P., & Singer, W. (1997). Visuomotor integration is associated with zero time-lag synchronization among cortical areas. *Nature, 385*(6612), 157-161. doi:10.1038/385157a0

Ruddy, K., Balsters, J., Mantini, D., Liu, Q., Kassraian-Fard, P., Enz, N., . . . Wenderoth, N. (2018). Neural activity related to volitional regulation of cortical excitability. *Elife, 7*. doi:10.7554/eLife.40843

Saramaeki, T., Mitra, S., & Kaiser, J. (1993). Finite impulse response filter design. *Handbook for digital signal processing, 4*, 155-277.

Seager, M. A., Johnson, L. D., Chabot, E. S., Asaka, Y., & Berry, S. D. (2002). Oscillatory brain states and learning: Impact of hippocampal theta-contingent training. *Proc Natl Acad Sci U S A, 99*(3), 1616-1620. doi:10.1073/pnas.032662099

Soekadar, S. R., Witkowski, M., Birbaumer, N., & Cohen, L. G. (2015). Enhancing Hebbian Learning to Control Brain Oscillatory Activity. *Cereb Cortex, 25*(9), 2409-2415. doi:10.1093/cercor/bhu043

Soekadar, S. R., Witkowski, M., Cossio, E. G., Birbaumer, N., & Cohen, L. G. (2014). Learned EEG-based brain self-regulation of motor-related oscillations during application of transcranial electric brain stimulation: feasibility and limitations. *Front Behav Neurosci, 8*, 93. doi:10.3389/fnbeh.2014.00093

Thut, G., Bergmann, T. O., Fröhlich, F., Soekadar, S. R., Brittain, J. S., Valero-Cabré, A., . . . Herrmann, C. S. (2017). Guiding transcranial brain stimulation by EEG/MEG to interact with ongoing brain activity and associated functions: A position paper. *Clin Neurophysiol, 128*(5), 843-857. doi:10.1016/j.clinph.2017.01.003

Thut, G., Schyns, P. G., & Gross, J. (2011). Entrainment of perceptually relevant brain oscillations by non-invasive rhythmic stimulation of the human brain. *Front Psychol, 2*, 170. doi:10.3389/fpsyg.2011.00170

Wach, C., Krause, V., Moliadze, V., Paulus, W., Schnitzler, A., & Pollok, B. (2013). The effect of 10 Hz transcranial alternating current stimulation (tACS) on corticomuscular coherence. *Front Hum Neurosci, 7*, 511. doi:10.3389/fnhum.2013.00511

Witkowski, M., Garcia-Cossio, E., Chander, B. S., Braun, C., Birbaumer, N., Robinson, S. E., & Soekadar, S. R. (2016). Mapping entrained brain oscillations during transcranial alternating current stimulation (tACS). *Neuroimage, 140*, 89-98. doi:10.1016/j.neuroimage.2015.10.024

Zrenner, C., Galevska, D., Nieminen, J. O., Baur, D., Stefanou, M.-I., & Ziemann, U. (2020). The shaky ground truth of real-time phase estimation. *Neuroimage*, 116761.